Journal of Inclusion Phenomena and Macrocyclic Chemistry (2005) 51: 121–136
DOI 10.1007/s10847-004-0912-z

Review Article

Peptide β-Bend and 3_{10}-Helix: from 3D-Structural Studies to Applications as Templates

CLAUDIO TONIOLO[1,*], MARCO CRISMA[1], FERNANDO FORMAGGIO[1], CRISTINA PEGGION[1], QUIRINUS BROXTERMAN[2] and BERNARD KAPTEIN[2]
[1]*Institute of Biomolecular Chemistry, CNR, Department of Chemistry, University of Padova, 35131 Padova, Italy;*
[2]*DSM Pharma Chemicals, Advanced Synthesis and Catalysis, P.O. Box 18, 6160 MD Geleen, The Netherlands*

(Received: 29 April 2004; accepted in final form: 11 May 2004)

Key words: β-bend, catalysis, donor–acceptor interaction, 3_{10}-helix, host–guest chemistry, macrocyclization, peptide conformation, C^{α}-tetrasubstituted α-amino acids

Abstract

The 3_{10}-helix is a relatively common secondary structure motif in peptides and proteins. Its building block is one of various types of β-bend conformation which comprises an N^{α}-acylated dipeptide alkylamide system. A complete 3D-structural characterization of this ternary helix has been achieved, thus allowing its unambiguous discrimination from the closely related α-helix. Recent applications of rigidified peptide β-bends and 3_{10}-helices as templates for investigations in synthetic organic chemistry (macrocyclization, catalysis), host–guest chemistry (molecular recognition), and physical chemistry (donor–acceptor interaction) will be discussed.

Abbreviations: Ac – acetyl; Agl – C^{α}-allylglycine; Aib – α-aminoisobutyric acid (or $C^{\alpha,\alpha}$-dimethylglycine); (αMe)Phg – C^{α}-methyl, C^{α}-phenylglycine; (αMe)Val: C^{α}-methyl valine; Api – 4-amino-4-carboxypiperidine; ATANP – 2-amino-3-[1-(1,4,7-triazacyclononane)] propanoic acid; Bin: 2′,1′:1,2;1″,2″:3,4-dinaphthcyclohepta-1,3-diene-6-amino-6-carboxylic acid; Boc – *tert*-butyloxycarbonyl; Bpa – *para*-benzoyl-phenylalanine; Bz – benzoyl; DMSO – dimethylsulfoxide; ESR – electron spin resonance; Fmoc – fluoren-9-ylmethyloxycarbonyl; hhMag, homo-homo-Mag; hMag – homo-Mag;Mag – C^{α}-methyl, C^{α}-allylglycine; NHBzl – benzylamino; NHMe – methylamino; NH*tBu*: *tert*-butylamino; OMe – methoxy; O*t*Bu: *tert*-butoxy; *p*BrBz – *para*-bromobenzoyl; Z: benzyloxycarbonyl; RCM – ring-closing metathesis; TEMPO: 2,2,6,6-tetramethylpiperidinyl-1-oxy; TOAC – 2,2,6,6-tetramethylpiperidine-1-oxy-4-amino-4-carboxylic acid; Tren – *tris*-(2-aminoethyl)amine

Introduction

A deep understanding of the detailed nature and mechanism of physico-chemical interactions between two probes or between two host functionalities and a guest (e.g. a substrate) molecule depends heavily upon our ability to appropriately design and successfully synthesize conformationally constrained 3D-structural platforms (templates) the intercomponent geometry of which (either rigorously rigid or able to undergo destructuration, if required, but always precisely tunable) would be well defined. To this goal we are currently actively working by exploiting stable, short peptide templates based on achiral and/or chiral C^{α}-tetrasubstituted α-amino acids (initial hints to this line of research were provided by our original crystallographic work on various peptides each characterized by two pendant, aromatic moieties [1]). These building blocks are known to force the peptides to predominantly fold into β-bends [2] or 3_{10}-helical conformations [3]. The systems under investigation also involve two suitable functional groups part of or covalently linked to amino acid side chains. By increasing the number of intervening residues the distance and relative orientation of the two side-chain groups can be easily modulated.

This review article highlights the 3D-structural details of the β-bend and 3_{10}-helical conformations and their recent applications as molecular templates in studies of macrocyclization reactions, catalysis, molecular recognition, and donor–acceptor interactions.

The β-bend and the 3_{10}-helix

Beside the classical α-helix and pleated β-sheet conformations, the only other principal long-range structure that occurs significantly in peptides (particularly in peptaibols [4]) and in proteins is the 3_{10}-helix [3]

*Author for correspondence. E-mail: claudio.toniolo@unipd.it

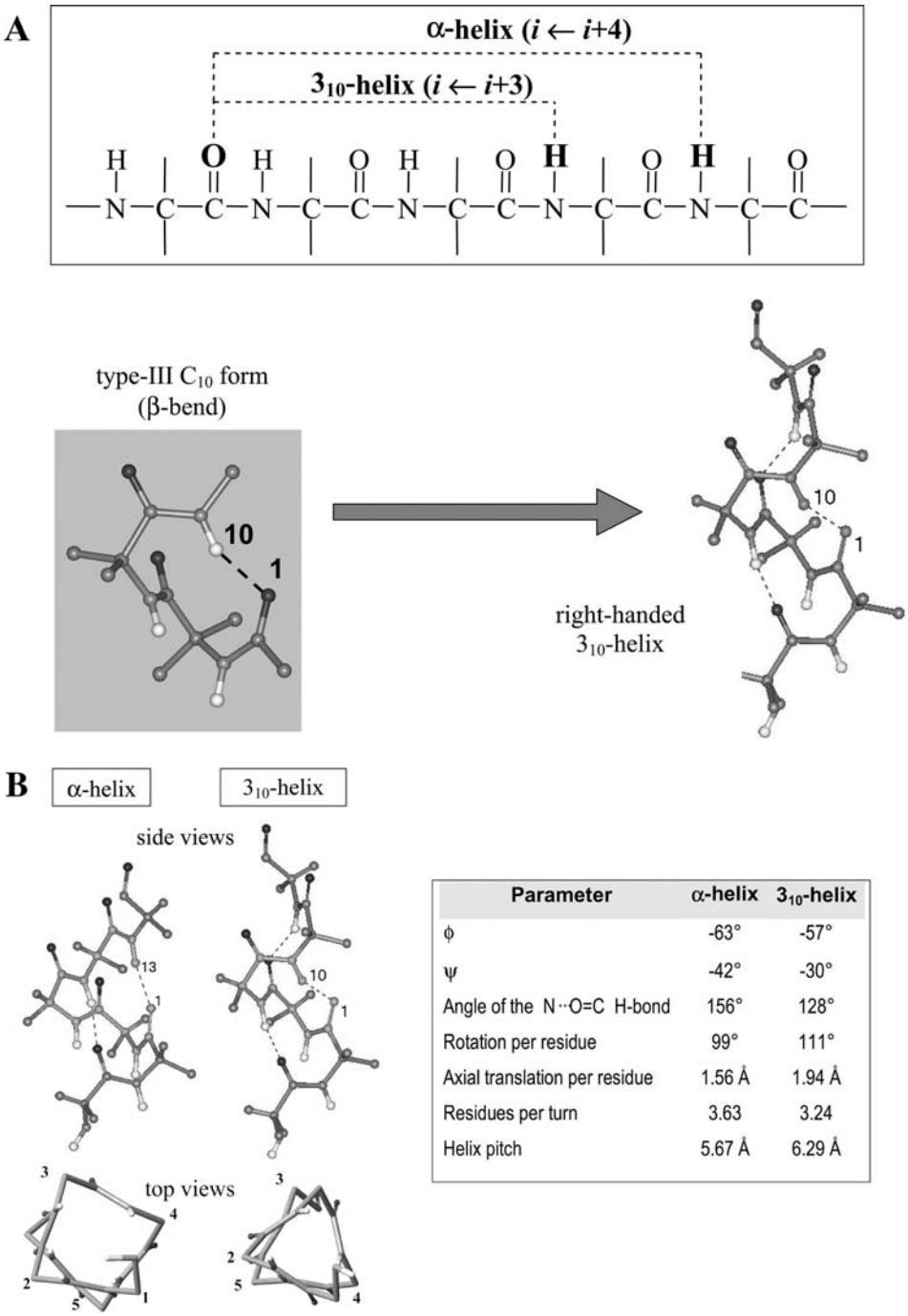

Figure 1. (A, B) Intramolecular C═O···H─N H-bonds, molecular models and 3D-structural parameters for the 3_{10}- and α-helices.

(Figure 1). Interestingly, this structure was first proposed by Taylor as early as in 1941 [5], 10 years before the α-helix [6]. The ternary 3_{10}-helix (or, more appropriately, the 3.0_{10}-helix [7]), being characterized by three amino acids per turn and ten atoms in the pseudo-ring formed by the intramolecular C═O···H─N H-bond (type III C_{10} form or *β*-bend [2]) (Figure 1) is more tightly bound and more elongated than the α-helix (3.6_{13}-helix) [3a]. The backbone torsion angles of the right-handed 3_{10}-helix ($\phi = -57°$, $\psi = -30°$) are within the same region of the conformational map as those of the α-helix ($\phi = -63°$, $\psi = -42°$). However, the intramolecular C═O···H─N H-bonding schemes are significantly different in the two helices, being of the $i \leftarrow i + 3$ type in the 3_{10}-helix, while of the $i \leftarrow i + 4$ type (helical C_{13}-form or α-bend [8]) in the α-helix.

3_{10}-Helices are not rare in globular proteins

A long polypeptide chain formed by C^{α}-trisubstituted α-amino acid residues in the 3_{10}-helix conformation is less stable than in the α-helix conformation. Indeed, its van der Waals energy is less favorable (it has several close, although not forbidden, short contacts) and the

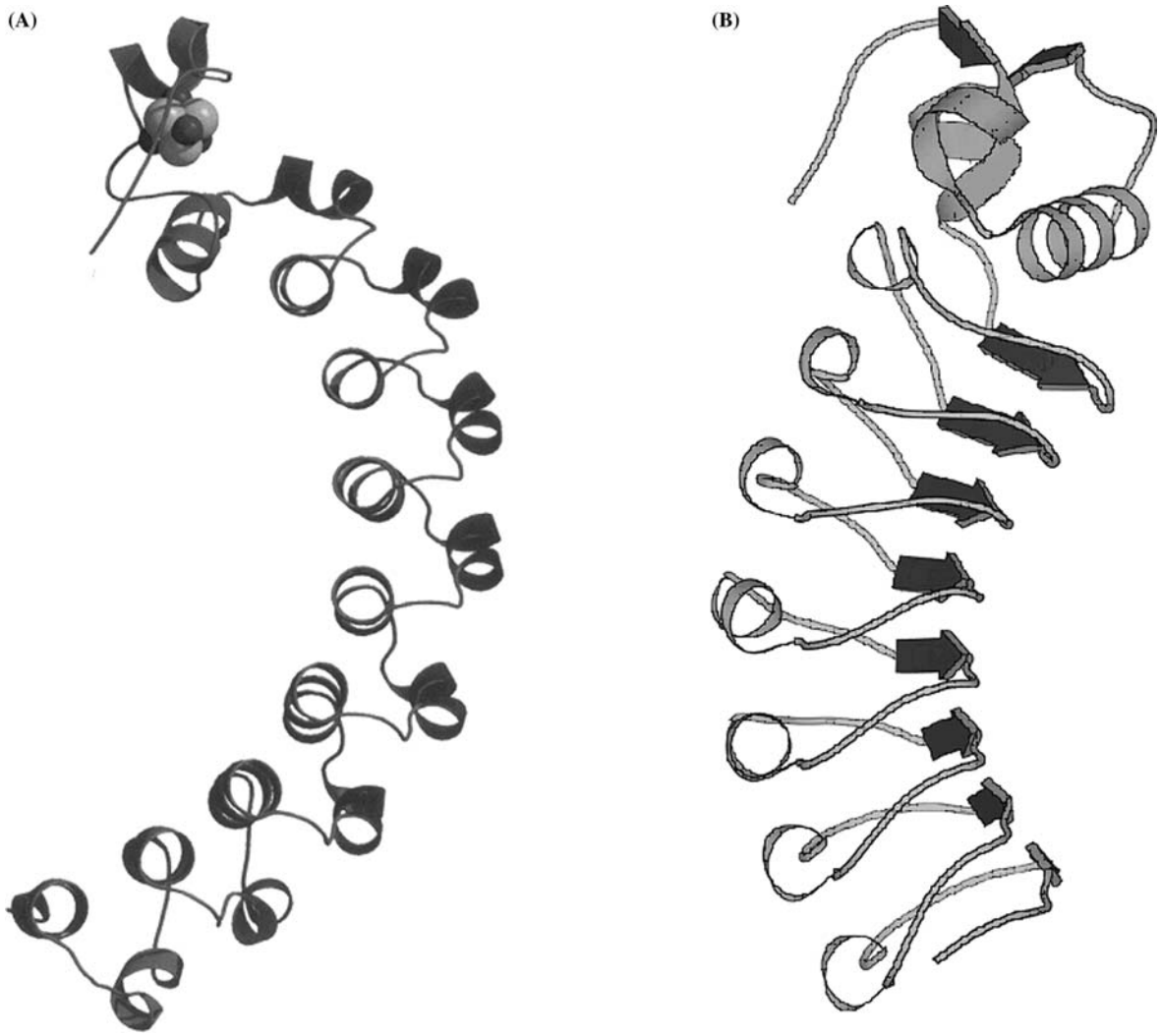

Figure 2. (A) The $\alpha/3_{10}$-helix motif of the Leu-rich repeat variant protein from *Azotobacter vinelandii* (the 3_{10}-helices are on the external, convex face) [10c]. (B) The 3_{10}-helix/β-sheet motif of the *L. monocytogenes* protein internalin B containing tandem Leu-rich repeats [10a,b].

H-bond geometry is not optimal [9]. Thus, for many years it was considered unlikely that long stretches of 3_{10}-helix would be observed. However, there is no disallowed region of the conformational (ϕ, ψ) space completely separating these two regularly folded secondary structures. Thus, the α-helix may be gradually transformed into a 3_{10}-helix (and vice versa) maintaining a nearly helical conformation of the chain throughout. Further, if one of the conformations should turn out to be impossible (say, as a result of side-chain interactions), the main chain may slip into the other conformation. In fact, the 3_{10}-helix appears to derive its importance mainly from its proximity in the conformational energy map to the more stable α-helix. Thus, a role of the 3_{10}-helix as an important intermediate in the mechanism of folding of α-helical proteins may be envisaged [3e,f].

In agreement with the above observations Barlow and Thornton [3b] surveyed all helices that were found in 57 of the globular protein crystal structures known up to December 1987 and showed that 3.4% of the residues are involved in 3_{10}-helices (about 10% of the total helical residues). These 3_{10}-helices are generally irregular; they have a larger radius and a smaller pitch than expected, with mean ϕ and ψ values of $-71°$ and $-18°$, 3.2 mean number of residues per turn, and a pitch value of 5.8 Å. The majority of known 3_{10}-helices are short (the mean length is 3.3 residues, i.e. one turn of helix) and 24% of 3_{10}-helices occur as an N- or a C-terminal extension to an α-helix.

More recently, significant improvements in atomic resolution have allowed protein crystallographers to detect a number of 3_{10}-helical segments, some of them as long as 7–12 residues. Two spectacular examples of $\alpha/3_{10}$-helix and 3_{10}-helix/β-sheet mixed motifs, occurring in Leu-rich repeat proteins, are shown in Figure 2 [10].

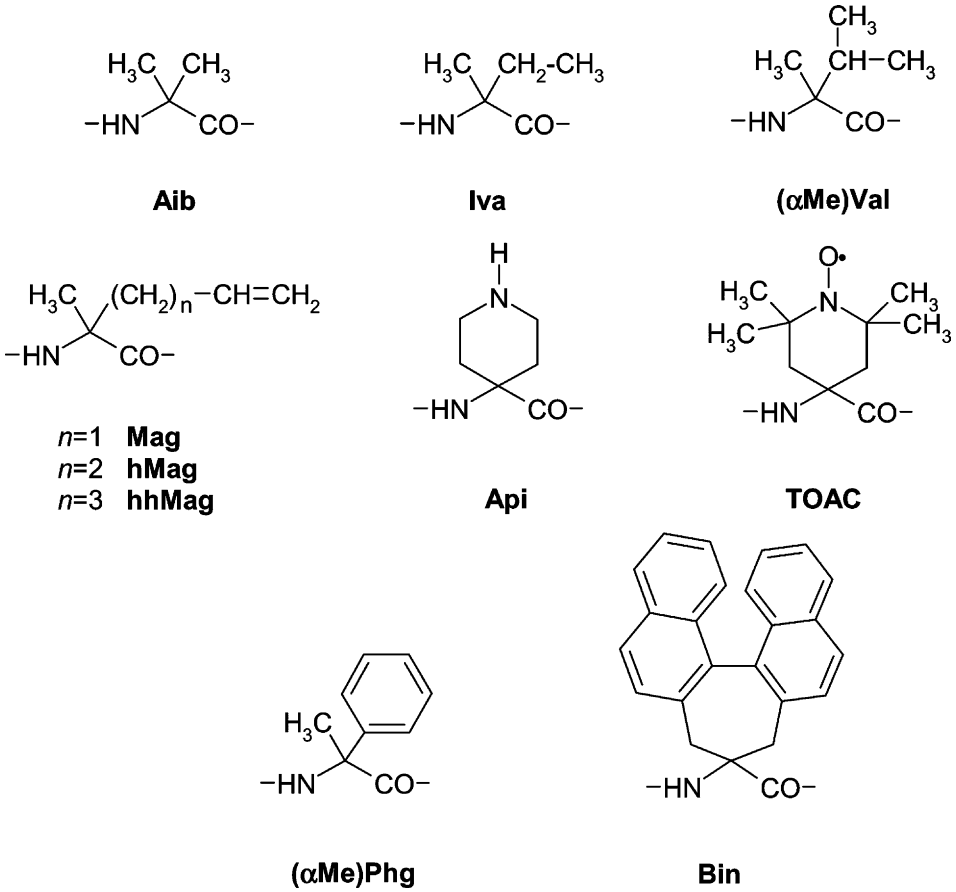

Figure 3. The C^{α}-tetrasubstituted α-amino acids discussed in this work.

3_{10}-Helices are common in peptides rich in C^{α}-tetrasubstituted α-amino acids

In 1971 Marshall [11] used conformational energy calculations to show that Aib (Figure 3), the prototype of achiral C^{α}-tetrasubstituted α-amino acids, can promote the onset of helices, due to steric interactions involving the *gem*-methyl groups linked to the α-carbon. Since 1978 [12a], by taking advantage of the extremely high crystallinity of peptides rich in C^{α}-tetrasubstituted α-amino acids, we and others have solved the X-ray diffraction structures of numerous Aib-based short model peptides and have shown that they form 3_{10}-helical structures [3c, 12b]. Figure 4 illustrates the molecular structure of an N- and C-blocked homodecapeptide, the second longest regular polypeptide 3_{10}-helix (almost three complete turns) described so far at atomic resolution [13a,b]. The X-ray diffraction structure of Z-$(Aib)_{11}$-O*t*Bu has recently been solved [13c].

In 1991, we carried out a general survey of the 32 3_{10}-helices experimentally observed in the high-resolution, single crystal, X-ray diffraction determinations of peptides, the atomic coordinates of which were available at that time [3a]. In parallel, a total of 22 α-helical, Aib-rich peptides (to the hexadecapeptide level) were also analyzed. A number of interesting conclusions were drawn from these data. The minimal main-chain length required for a peptide to form an α-helix corresponds to seven residues [3c, 14]. By contrast, there is no critical main-chain length dependence for 3_{10}-helix formation, i.e. incipient 3_{10}-helices are formed at the lowest possible level (the N^{α}-blocked tripeptide) [15]. An N- and C-blocked -(Aib-L-Ala)$_3$- peptide gives a regular 3_{10}-helix, but an -(Aib-L-Ala)$_4$- peptide is folded in a predominant α-helix. In peptides of eight or more residues the α-helix is preferred over the 3_{10}-helix if the percentage of Aib residues does not exceed 50%. However, one or two 3_{10}-helical residues may be observed at either end of the α-helical stretch (a short 3_{10}-helix tightens up the ends of the α-helix by moving the related peptide groups nearer to the axis). The average number of α-helical residues in undeca- and longer peptides is seven (two turns). A comparison of the side-chain staggering for a 3_{10}- and an α-helix built up with the parameters given in Figure 1B is shown in Figure 5 [3a].

The crystallographic study of C^{α}-tetrasubstituted α-amino acid-rich peptides has allowed us to characterize the 3_{10}-helix in great detail (at atomic resolution). In particular, the ϕ, ψ angles observed in peptides (−57°, −30°) differ substantially from those reported for proteins (−71°, −18°) [3b]. In our view, this difference is not related to the effect of the Aib residues, but rather

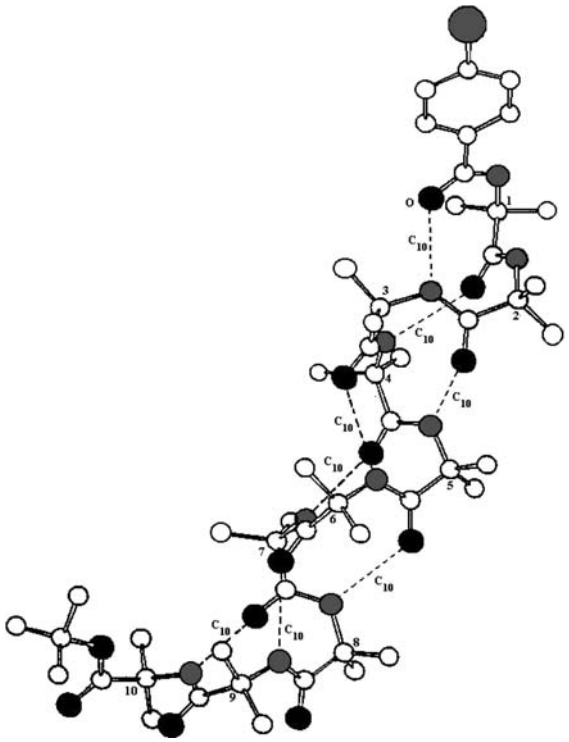

Figure 4. X-Ray diffraction structure of the 3_{10}-helical, terminally-blocked decapeptide *p*BrBz-$(Aib)_{10}$-O*t*Bu with eight $i \leftarrow i+3$, intramolecular C═O···H─N H-bonds (giving rise to eight β-bends) represented as dashed lines [13a,b].

to the observation that the 3_{10}-helices in peptides are longer and more regular than those occurring in proteins (the mean length is 4.9 *versus* 3.3 residues). By contrast, the number of residues per turn in peptides (3.24) is close to that observed in proteins (3.2), a value intermediate between those of the theoretical 3.0_{10}-helix and the $\alpha(3.6_{13})$-helix. In the 3_{10}-helix, the side chains on successive turns are exactly eclipsed since there is an integer number of residues per turn. However, the experimentally observed non-integer number of residues per turn does not line up side chains, thereby inducing a slightly staggered, energetically more favorable disposition.

In recent years, we have experimentally characterized the right-handed peptide 3_{10}-helix in solution. In a structure-supporting solvent, this helix is fully developed at the octapeptide level [16a]. Standard 3_{10}-helix spectra are now available for a number of physico-chemical techniques, including IR absorption [16a, b], vibrational CD [16c], electronic CD [16d,e], and NMR [16f,g]. More specifically: (i) In the IR spectral region the N─H (amide A) and C═O (amide I) stretching absorption bands are seen at 3350–3320 and 1662 cm^{-1}, respectively. The amide II band occurs at about 1530 cm^{-1}. (ii) In the vibrational CD spectrum the amide I band is a nearly conservative, positive couplet, negative to higher energy. The zero-crossing point is at 1665 cm^{-1}. The amide II band (near 1515 cm^{-1}) is negative and more intense than the amide I band. (iii) In the electronic CD spectrum, a negative band at 204–207 nm is accompanied by a shoulder centered near 222 nm. The ratio $R = [\theta]_{222}/[\theta]_{205}$ is 0.3–0.4. The positive maximum at 195 nm is very weak. A further negative maximum is visible near 185 nm. (iv) In the classical $CDCl_3$/DMSO and $CDCl_3$/TEMPO titrations by ^1H NMR of a 3_{10}-helix forming peptide, only the first two (from the N-terminus) NH protons are sensitive to the external perturbing agent. Typical NOE effects for a 3_{10}-helix are of the $d_{\alpha N}$ $(i, i+2)$ type. Surprisingly, a very slow 3_{10}-helix $\rightarrow$ α-helix conversion has been experimentally determined in a terminally blocked L-(αMe)Val (Figure 3) homo-octapeptide [16c,g]. Low peptide concentration, high solvent polarity, and high temperature

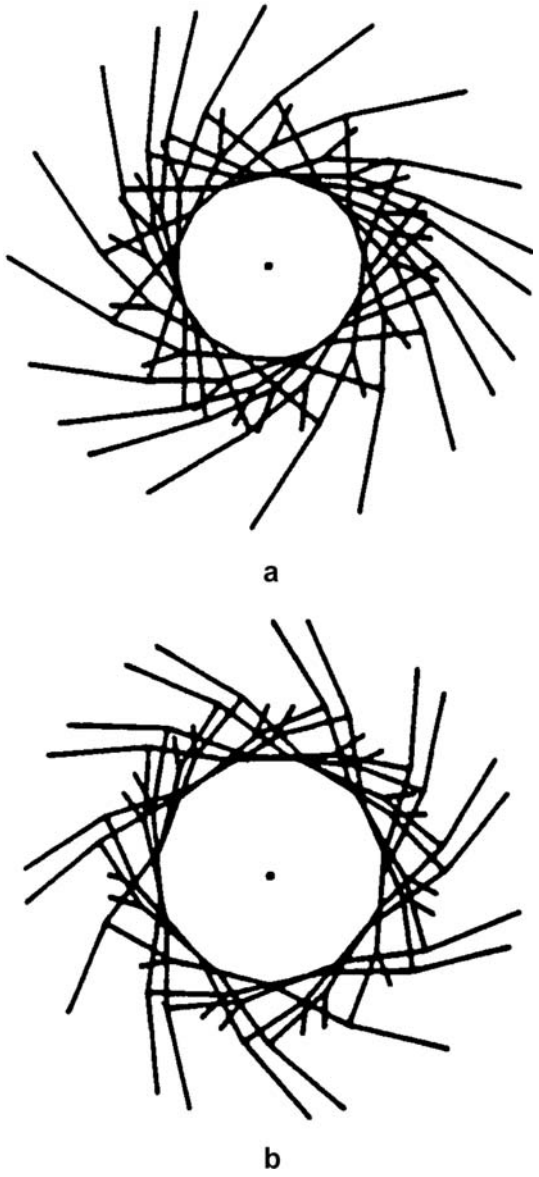

Figure 5. A comparison of the side-chain staggering for (a) a 3_{10}-helix and (b) an α-helix built up with the helical parameters given in Figure 1B. The two helices are viewed down the helix axis, with the C^{α}─C^{β} bonds projecting radially outwards [3a].

THE 3_{10}-HELIX. HISTORICAL BACKGROUNDS

EARLY DAYS (1941-1966)

1941	Taylor	first proposal
1943	Huggins	first model
1950	Bragg, Kendrew, Perutz	discussed
1952	Pauling	discussed
1953	Donohue	model
1962	Blout, Fasman Elliott, Bradbury	discussed
1965	De Santis, Liquori	conformational energy calculations; $(Ala)_n$
1966	Ramachandran, Venkatachalam	hard-sphere diagram; $(Ala)_n$

THE GREAT EXPLOSION (1977-1984)

Marshall, Duax, Smith	X-ray; solution; Aib peptides
Balaram	X-ray; solution; first fully developed 3_{10}-helical (Aib) peptide
Jung	X-ray; solution; Aib peptides
Karle, Flippen-Anderson	X-ray; Aib peptides
Toniolo, Benedetti	X-ray; solution; Aib peptides
Richards	X-ray; first natural Aib peptide
Malcolm	electron diffraction; poly $(Aib)_n$
Krimm	IR; poly $(Aib)_n$
Scheraga, Némethy	conformational energy calculations; $(Aib)_n$
Sasisekharan, Venkataram Prasad	conformational energy calculations; $(Aib)_n$

RECENT WORK

1988	Barlow, Thornton	statistical analysis (X-ray) in proteins
1991	Toniolo, Benedetti	statistical analysis (X-ray) in peptides; first review article
1992	Neet	statistical analysis (X-ray) in proteins
1999, 2002, 2003	Basu, Chakrabarti	statistical analysis (X-ray) in proteins
1999	Millhauser	review article

Figure 6. The 3_{10}-helix: historical backgrounds.

are all parameters found to stabilize the α-helical structure. In two terminally blocked Aib- or L-(αMe)Val/Aib-rich oligopeptides this conformational transition has been shown to be reversible (temperature- or solvent-driven molecular springs) [17].

The history of 3_{10}-helix, from its first proposal to recent review articles, is summarized in Figure 6.

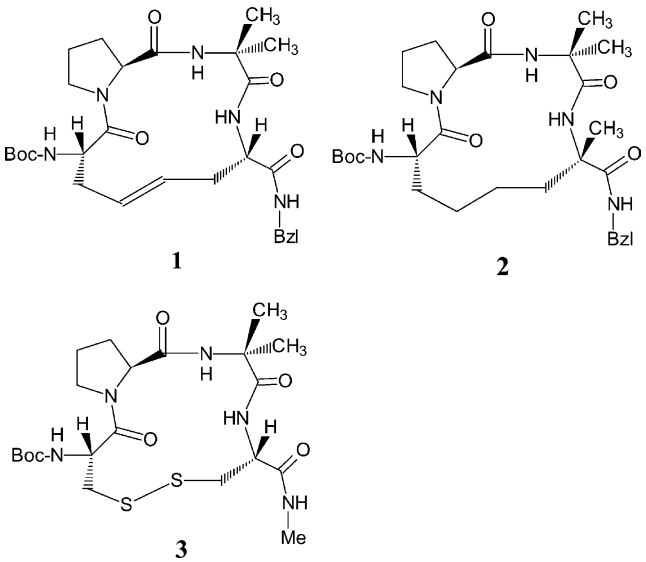

Figure 7. Representations of the Grubbs' alkene-stabilized, L-Pro-Aib- cyclized, β-bend peptide (1) [18d], our alkane-stabilized, -L-Pro-Aib- cyclized, β-bend peptide (2) [18e], and the Balaram's disulfide-stabilized, -L-Pro-Aib- cyclized, β-bend peptide (3) [18g].

The β-bend and the 3_{10}-helix as templates

Macrocyclization

Verdine and coworkers [18a], using a large set of C^{α}-methylated, side-chain alkene-containing α-amino acids (e.g. the Mag, hMag, and hhMag residues shown in Figure 3), clearly demonstrated that it is possible to cyclize *via* RCM an unperturbed α-helical peptide at both i, $i+4$ and i, $i+7$ relative positions provided that the olefinic side chains have an appropriate length. In an otherwise all-L peptide, if both olefinic residues at the i, $i+4$ positions are of either the L- or the D-configuration, the smallest ring system formed has 20 atoms. Moreover, in an otherwise all-L peptide, if the olefinic residues at the i, $i+7$ positions are one of the L- and the other of the D-configuration, the smallest ring system formed has 31 atoms.

Grubbs and coworkers [18b,c] synthesized cyclic peptides of 21 and 23 atoms in high yields *via* RCM of two olefinic L-residues located at the i, $i+4$ positions. The 3_{10}-helical structure of the peptide reagent seems to be preserved in the cyclic product. However, it is worth pointing out that in a 3_{10}-helix the intramolecular distance between residues i and $i+4$ is significantly higher than the i, $i+3$ distance.

In the Verdine [18a] and Grubbs [18b,c] peptides both olefinic residues are *internal* to the helical systems. Grubbs and coworkers [18d] were also able to cyclize *via* RCM three peptides forming one or two consecutive β-bends, each with two Agl (i, $i+3$) residues (for one example, see peptide **1** in Figure 7). The resulting cyclic

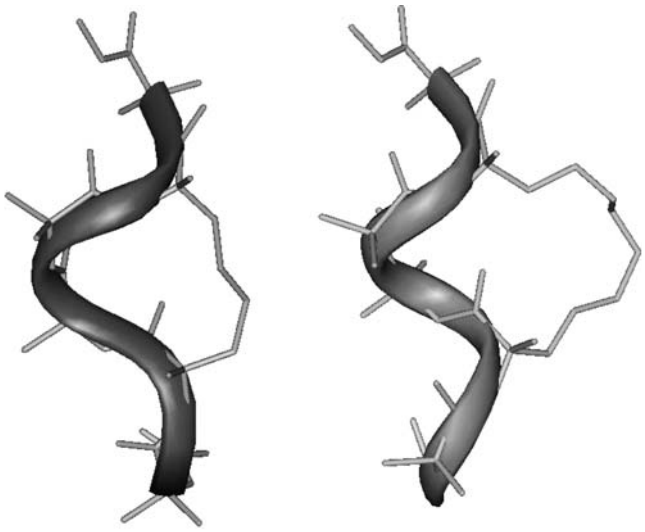

Figure 8. Minimum-energy models for the two hexapeptides Ac-Aib-Xxx-(Aib)$_2$-Xxx-Aib-NHMe with (*i*, *i* + 3) Xxx residues L-Mag (structurally perturbed 3_{10}-helix; left) or L-hhMag (unperturbed 3_{10}-helix; right) [18h].

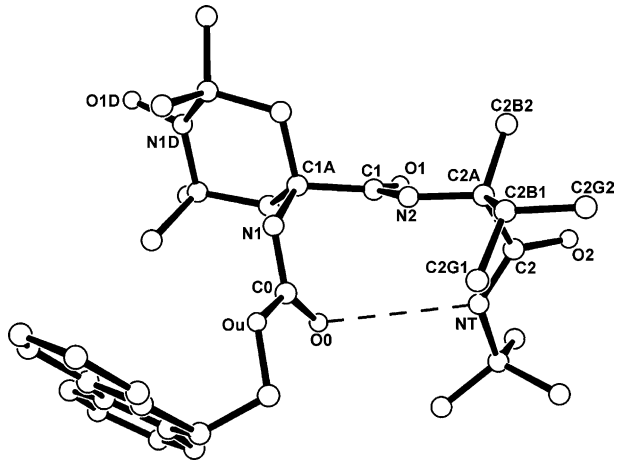

Figure 9. X-Ray diffraction structure of Fmoc-TOAC-L-(αMe) Val-NH*t*Bu. The intramolecular C═O···H─N H-bond is represented by a dashed line [19].

system is small (14 atoms). Analogous results were reported by our groups [18e] with a turn-forming, Agl/Mag *i*, *i*+3 (peptide **2** in Figure 7) and by Pernerstorfer *et al*. [18f]. It is very important to note that in all these cases the N-terminal C^{α}-tetrasubstituted Agl (or related) residue is *outside* the rigid, central β-bend structure. We also reported the failure to achieve RCM in several β-bend/3_{10}-helical, Mag/Mag *i*, *i*+3 peptides (in these compounds both Mag residues are internal to the turn/helices), i.e. the 14-atom ring system is not formed. At this point, it is relevant to mention that in the crystal state the Cys1 residue of the related, disulfide tethered Boc-L-Cys-L-Pro-Aib-L-Cys-NHMe peptide (peptide **3** in Figure 7), that also forms a 14-atom ring system, is *outside* the two consecutive β-bend structures [18g].

More recently, in addition to experimentally and theoretically confirming the β-bend propensity for the allyl-based, C^{α}-tetrasubstituted α-amino acid Mag, our conformational energy computations significantly expanded the picture of RCM in bend/helical peptides by indicating that two *i*, *i*+3 side chains of the type-─$(CH_2)_3$─CH═CH_2 (hhMag or hhAgl) represent the minimal length requirement to achieve RCM on an unperturbed 3_{10}-helix (Figure 8) [18h]. In these compounds 18-atom ring systems are formed. It is gratifying that these theoretical findings indirectly support the experimental results discussed above.

Catalysis

(i) Considerable recent interest has been focused on the enantioselective oxidation of racemic alcohols with chiral nitroxyl catalysts. In this connection, we have recently shown that conformationally rigid, stable β-bend forming, very short peptides based on TOAC (Figure 3), e.g. Fmoc-TOAC-L-(αMe)Val-NH*t*Bu (Figure 9), are valuable, enantioselective catalysts in chemical oxidations and, although less efficient, in electrochemical oxidations as well [19]. Longer helical structures seem not to be required. Large aromatic or aliphatic N- and C- blocking groups and the N-terminal positioning of TOAC have a positive effect on the efficiency. We have explained these experimental findings on the basis of computer models for the intermediate adducts between the chiral dipeptide amide N-oxoammonium mediator and the enantiomeric secondary alcohol substrates (Figure 10). The identity of the fast reacting alcohol enantiomer has been correctly predicted.

However, it is clear that the experimental selectivity factors (in the range 2.3–2.7 for our best catalysts, which corresponds to a free-energy difference of only about 0.5 kcal mol^{-1}), are far from optimal, particularly in view of the high conversion (81–83%) achieved in enantioselective chemical oxidation experiments. It is our contention that these results are related to the only chiral centre of the catalyst, that is the (αMe)Val α-carbon atom, being too far removed from the TOAC oxidation site. Current attempts in our laboratories are aimed at designing and synthesizing chiral TOAC analogues.

(ii) Miller and coworkers [20] recently expanded the field of peptide catalysts by showing that His(π-Me) peptides can be used for the kinetic resolution of racemic alcohols. As most of these peptides are characterized by an Aib residue, they are strongly biased towards a β-bend conformation in solution which decreases catalyst flexibility. Indeed, all of the tripeptide amide and the tetra- and pentapeptide ester very active catalysts examined share the common feature of a β-hairpin (a β-bend followed by a short β-sheet) conformation, in which a type-II′ β-bend, generated by a -D-Pro-Aib-(*i*+1, *i*+2) sequence, is further stabilized by an

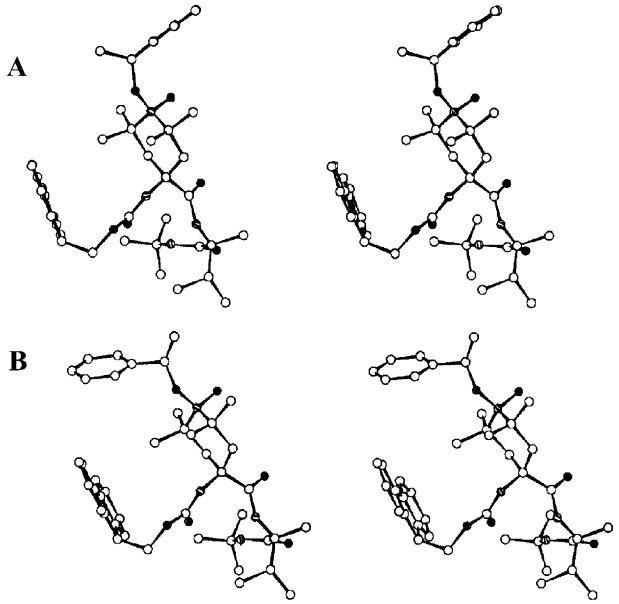

Figure 10. Stereoviews of the minimum energy structures of the diastereomeric intermediates between Fmoc-TOAC-L-(αMe)Val-NH*t*Bu and the substrate (*S*)-1-phenylethanol (A) or (*R*)-1-phenylethanol (B), with addition of the alcohol on the TOAC ring side close to the Fmoc group [19].

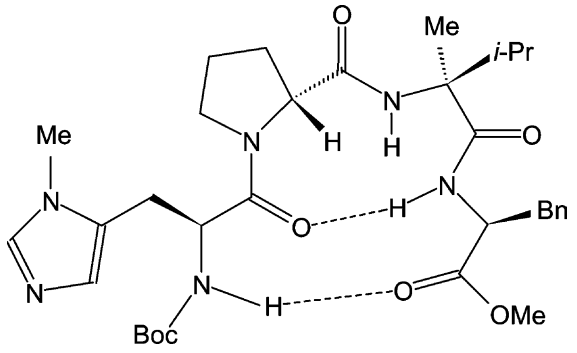

Figure 11. Preferred (β-hairpin) conformation of the tetrapeptide Boc-L-His(π-Me)-D-Pro-(L-αMe)Val-L-Phe-OMe in $CDCl_3$ solution (F. Formaggio *et al.*, submitted for publication).

(*i*)N—H···O=C(*i*+2) intramolecular H-bond. These authors also demonstrated that: (i) the Aib residue at position *i*+2 of the β-bend can be replaced by any of other *achiral* members of its class with only a limited detrimental effect on resolution efficiency [20j], and (ii) the Phe residue at position *i*+3 of the β-bend cannot be replaced by any of the helicogenic C^{α}-tetrasubstituted α-amino acid residues without an almost complete loss of enantioselectivity [20j].

We have further extended the investigation on the Miller tetrapeptide prototype Boc-L-His(π-Me)-D-Pro-L-(αMe)Val-NH*t*Bu (F. Formaggio *et al.*, submitted for publication) by synthesizing and studying two tetrapeptide analogs with the *achiral* Aib residue replaced by a *chiral* amino acid of its class with different side-chain bulkiness and helical screw-sense propensity [L-(αMe)-Val is remarkably bulkier and more strongly biased toward the right-handed helical structure, appropriate for the *i*+2 position of a type-II′ β-bend, than L-Iva (Figure 3)] [12b]. We found that the transacylation reactivity is very sensitive to the steric hindrance of the residue at position *i*+2, rapidly decreasing from Aib to Iva and from Iva to (αMe)Val. However, both analogs are remarkably stereoselective with the L-(αMe)Val-based peptide catalyst being even more effective, although slightly, than the prototypical peptide. Also, our conformational analysis by FT-IR absorption and ^{1}H NMR lent credence to the close correlation between catalyst stereoselection efficiency and a β-hairpin, rigidified structure (Figure 11), as proposed by Miller and coworkers [20].

In the capture of the acylating reagent by the His(π-Me) nucleophilic side chain, these authors invoked the occurrence of two diastereomeric transition states of diverging stability on the basis of differential H-bonding interactions of alcohol substrate enantiomers with the

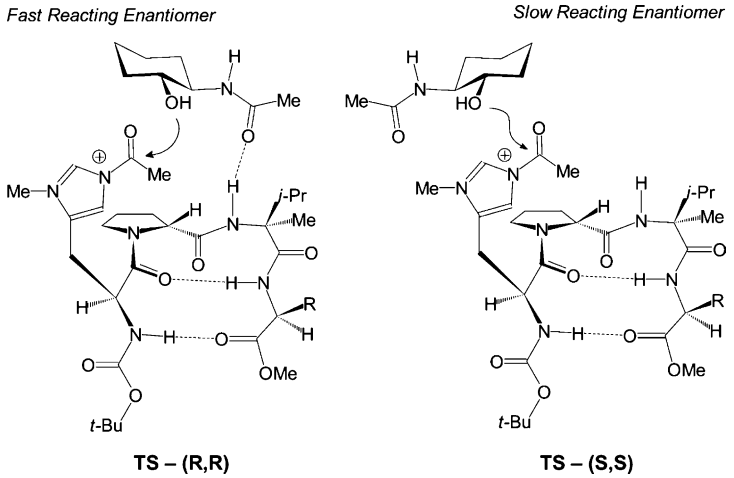

Figure 12. Transition state proposed for the fast-reacting enantiomer [TS(*R*,*R*)] and the slow-reacting enantiomer [TS(*S*,*S*)] in the asymmetric acetylation reaction catalyzed by the tetrapeptide Boc-L-His(π-Me)-D-Pro-(L-αMe)Val-L-Phe-OMe (F. Formaggio *et al.*, submitted for publication).

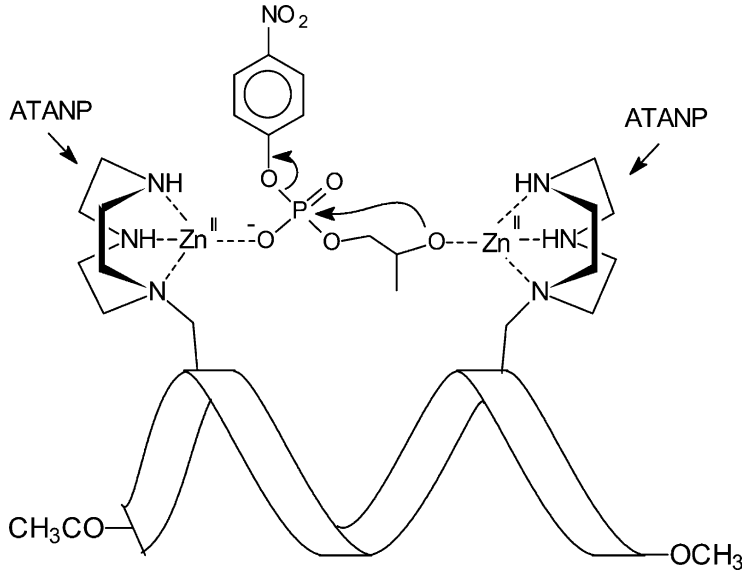

Figure 13. Proposed mechanism for the cleavage of 2-(hydroxypropyl)-*p*-nitrophenyl phosphate by the *bis*-Zn(II), ATANP-based helical heptapeptide complex [21a].

chiral environment generated by the highly folded tetrapeptide catalyst [20a,d]. In this connection the important role played by the Pro-Xxx secondary amide bond was also demonstrated [20h]. Our findings fit nicely into this reaction scheme and unambiguously confirm that β-bend formation (and its stabilization *via* β-hairpin) in the peptide catalyst is a prerequisite for excellent reactivity and stereoselectivity and that enhanced steric hindrance at position $i+2$ of the β-bend is not detrimental, or it might be even beneficial, for the stereoselection governed by the ancillary H-bonding interaction between the peptide catalyst and the racemic alcohol substrate (Figure 12).

Furthermore, our results on tetrapeptide Boc-L-His(π-Me)-D-Pro-Aib-L-(αMe)Phg-OMe indirectly support the contention that a β-hairpin template (not just a

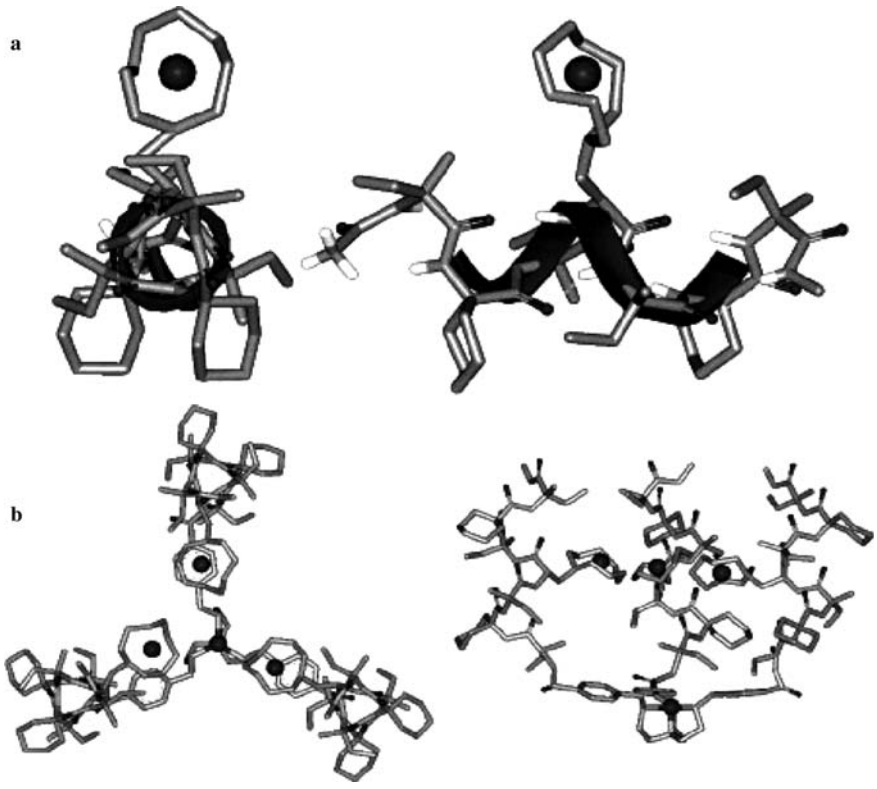

Figure 14. Top (left) and side (right) views of the molecular models of the Zn(II) complex of the Iva/Api/ATANP heptapeptide amide (a) and the tetrazinc complex of the Tren-based, *tris*-peptide template (b) [21d].

β-turn template) is strictly required for a peptide catalyst to exhibit significantly different rates in the acylation of the alcohol enantiomers. Indeed, as already reported by Jarvo *et al.* [20j], incorporation at position 4 of the β-bend of a C^{α}-tetrasubstituted α-amino acid, e.g. L-(αMe)Phg (Figure 3), with its propensity for a more or less extended structure weaker than that of L-Phe [12b] seems to reduce the population of conformers with the (His)N—H···O=C(Phe) intramolecular H-bond, thereby enhancing their conformational freedom and concomitantly decreasing peptide catalyst stereoselectivity.

In search of a shorter, industrially more attractive, peptide catalyst of this asymmetric acylation reaction. We have also synthesized and investigated the terminally protected dipeptide amides (F. Formaggio *et al.*, submitted for publication). In these compounds, long enough to generate an intramolecularly H-bonded β-bend but too short for β-hairpin formation, the nucleophilic His(π-Me) residue at position 1 is followed by a chiral C^{α}-tetrasubstituted α-amino acid. Again, we have noted a close relationship between peptide catalyst conformation and stereoselectivity in that, unfortunately, the population of β-bend conformers is quite limited in these dipeptide amides and their stereoselectivity is poor.

Taken together, our experimental findings underscore the points that a rigid, β-hairpin secondary structure is an element of paramount importance characterizing the platform required by a peptide to be an efficient stereoselective catalyst in the acylation reaction for alcohol resolution and that, in this connection, chiral C^{α}-tetrasubstituted α-amino acids may play a fundamental role.

(iii) A substantial weight of experimental evidence indicates that many metallohydrolases contain and

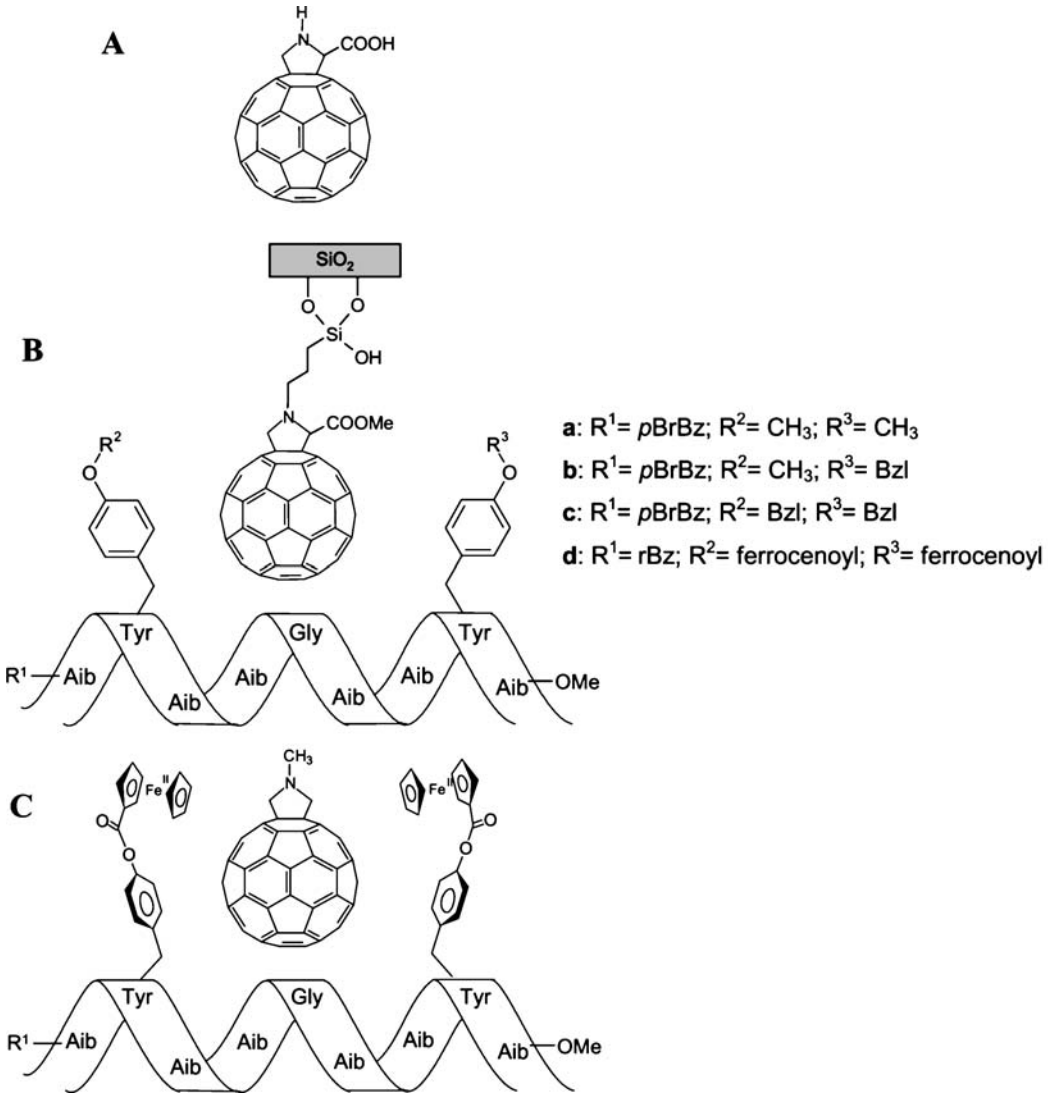

Figure 15. (A) The [60] fullero-3,4-proline α-amino acid. (B) The supramolecular complex formed by an N^{α}-silica-grafted [60] fullero-3,4-proline methyl ester and a series of 3_{10}-helical, Aib-rich nonapeptides [22b]. (C) The supramolecular complex formed by N-methylfulleropyrrolidine and the *bis*-ferrocenoyl nonapeptide [22c].

require a binuclear metal ion site for activity. These include enzymes able to cleave RNA and DNA. A number of research groups have reported suitably designed, simple dinuclear metal complexes quite effective in the cleavage of model substrate esters. In some cases these dinuclear complexes proved effective in the cleavage of RNA and, to a less extent, of DNA as well. This latter biopolymer is a quite challenging target because of its very sluggish reactivity under physiological conditions. In this connection we have recently shown that the dinuclear complex of heptapeptide Ac-Aib-L-ATANP-$(Aib)_2$-L-ATANP-$(Aib)_2$-OMe is active in catalyzing the intramolecular transphosphorylation of the RNA model substrate 2-hydroxypropyl-*p*-nitrophenyl phosphate [21a,b]. Analysis of the reaction mechanism indicated cooperativity between the two Zn(II) ions (Figure 13) but a weak binding of the substrate to the catalyst. We suspected that such a weak binding could be the reason for our inability to evidentiate any significant rate acceleration in the cleavage of the DNA model substrate bis-*p*-nitrophenyl phosphate. However, we argued that polyanionic DNA, a substrate for which the interaction with the metal centers could be emphasized, would be an accessible hydrolytic target. Indeed, a dinuclear Zn(II) complex of the 3_{10}-helical Aib/ATANP heptapeptide was shown to act as a powerful catalyst for the hydrolytic cleavage of plasmid DNA [21c]. The precise distance between the two metal centers, as defined by the pitch of the helix (6.3 Å), which matches that between two adjacent DNA phosphate groups, allows one to take advantage of the cooperation between the two Zn(II) ions in binding and performing the hydrolytic process.

By connecting three copies of the 3_{10}-helical heptapeptide H-L-Iva-Api-L-Iva-L-ATANP-L-Iva-Api-L-Iva-NHMe (Figure 14A) to a functionalized, Tren platform, a new *tris*-peptide template was obtained [21d]. This molecule is able to bind up to four metal ions (Cu^{II} or Zn^{II}): one in the Tren subsite and three in the ATANP azacyclononane subunits. The binding of the metals to the Tren platform induces a change from an open to a closed conformation in which the three short, helical peptides are aligned in a parallel manner with the azacyclononane units pointing inward within the pseudocavity (Figure 14B). This peptide template shows a peculiar behavior in the transphosphorylation of phosphate esters; the tetrazinc complex is a catalyst of the cleavage of 2-hydroxypropyl-*p*-nitrophenyl phosphate, whereas the free ligand is a catalyst of the cleavage of an oligomeric RNA sequence with selectivity for pyrimidine bases. In the case of the model phosphate, Zn(II) acts as a positive allosteric effector by enhancing the catalytic efficiency of the system. In the case of the polyanionic RNA substrate Zn(II) switches off the activity, thus behaving as a negative allosteric regulator. It is suggested that the opposite behavior of the catalyst induced by Zn(II) is associated with the change of conformation of the Tren platform, and consequently of the relative spatial disposition of the three linked, 3_{10}-helical peptides, that occurs after binding of the metal ion.

Host–guest chemistry

Rational design of Aib-based peptides was also utilized in molecular recognition studies. [60]Fullero-3,4-proline (Figure 15A) is the biggest unnatural α-amino acid and the first example of a protein residue (Pro) condensed to a 6,6-ring junction of the C_{60} sphere [22a]. An interesting application of fullero-proline derivatives is the preparation of a C_{60}-modified silica gel as a new stationary phase for HPLC column chromatography. A suitable aziridine, functionalized at the nitrogen atom with a trialkoxysilane group, was synthesized and allowed to react with C_{60}, affording the silicon-based compound shown in Figure 15B. Grafting was easily achieved by

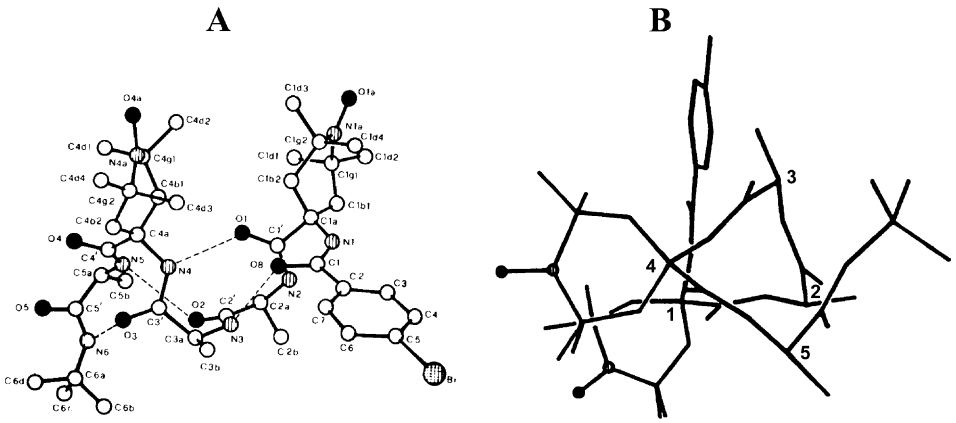

Figure 16. (A) X-ray diffraction structure of *p*BrBz-TOAC-$(L\text{-Ala})_2$-TOAC-L-Ala-NH*t*Bu with numbering of the atoms (side view). The intramolecular C═O···H─N H-bonds are represented by dashed lines [23a,b]. (B) Projection of the *p*BrBz-TOAC-$(L\text{-Ala})_2$-TOAC-L-Ala-NH*t*Bu molecule down the helix axis (top view). Position of a given amino acid in the peptide chain is indicated by a number on its C^{α}-atom. The N and O atoms of the two nitroxide groups are represented by dashed and full circles, respectively. The almost perfect triangular shape of the 3_{10}-helix stands out clearly [23b].

simple heating on toluene [22b]. The new chromatographic material was used in either organic or aqueous solution to investigate the binding affinities of potential hosts for the immobilized C_{60} core. In particular, the possibility of exploiting this stationary phase to study the interaction of host–guest systems in aqueous solvents is quite advantageous. Calixarenes and cyclodextrins of different size were selectively separated using the novel fullerene-doped silica gel HPLC column. Moreover, selective recognition was demonstrated by analyzing the interaction of the grafted fullerene with a series of rationally designed peptides forming cavities. In particular, Aib-rich nonapeptides which, according to our X-ray diffraction, IR absorption and NMR conformational analyses, fold into 3_{10}-helix and are characterized by two pendant hydrophobic residues (two side-chain substituted Tyr residues) separated by two helical turns (~12.5 Å), displayed chromatographic retention times that are related to the ability of the side chains to generate a cleft for the accommodation of a C_{60} molecule. The retention times were also related to the donor properties of the peptide side chains. It was indeed found that the peptides with either two benzyl (**c**) or two ferrocenoyl (**d**) side chains gave the most effective interactions.

The fact that peptide **d** possesses a high affinity for the [60]fullerene spheroid was also demonstrated by photophysical measurements [22c]. Our investigation confirmed that in a solvent of low polarity the ferrocenoyloxybenxyl walls of the peptide template do indeed host the *N*-methylfulleropyrrolidine molecule (Figure 15C). Upon photoexcitation the singlet excited state of *N*-methylfulleropyrrolidine is therefore primed for a rapid intra-complex deactivation by the ferrocenoyl groups. Conversely, in a more polar solvent mixture, which disfavors the formation of a host–guest complex. no evidence for intra-complex processes was obtained. An additional proof for the onset of the superstructure was provided by a mass spectrometric investigation in the gas phase. Compound **d** is, to our knowledge, the first peptide-based, (1:1) mini-receptor reported for [60]fullerene. In their classical paper Friedman *et al.* [22d] proposed that a [60]fullerene molecule could be sandwiched snugly into the hydrophobic cavity generated by the HIV protease dimer (1:2 stoichiometry).

A review article on fullerene-based amino acids and peptides, including their applications as guests to supramolecular chemistry, has recently been published [22e].

Donor–acceptor interaction

The C^{α}-tetrasubstituted α-amino acid TOAC is characterized by a saturated heterocyclic structure containing a paramagnetic probe (a nitroxide) stabilized by the presence of two contiguous tetrasubstituted carbon atoms [23a]. A very favorable property of TOAC over spin-labeled protein amino acids, the latter with a flexible link connecting the label to the peptide backbone, is its very restricted mobility due to C^{α} tetrasubstitution and hampered rotation about side-chains bonds, which is in turn related to the incorporation of the nitroxide and the C^{α}, C^{β}, and C^{γ} atoms into a cyclic moiety. Therefore, TOAC represents an extremely useful tool for the exploitation of the sensitive ESR [23] and the related CIDEP [24] techniques in peptide

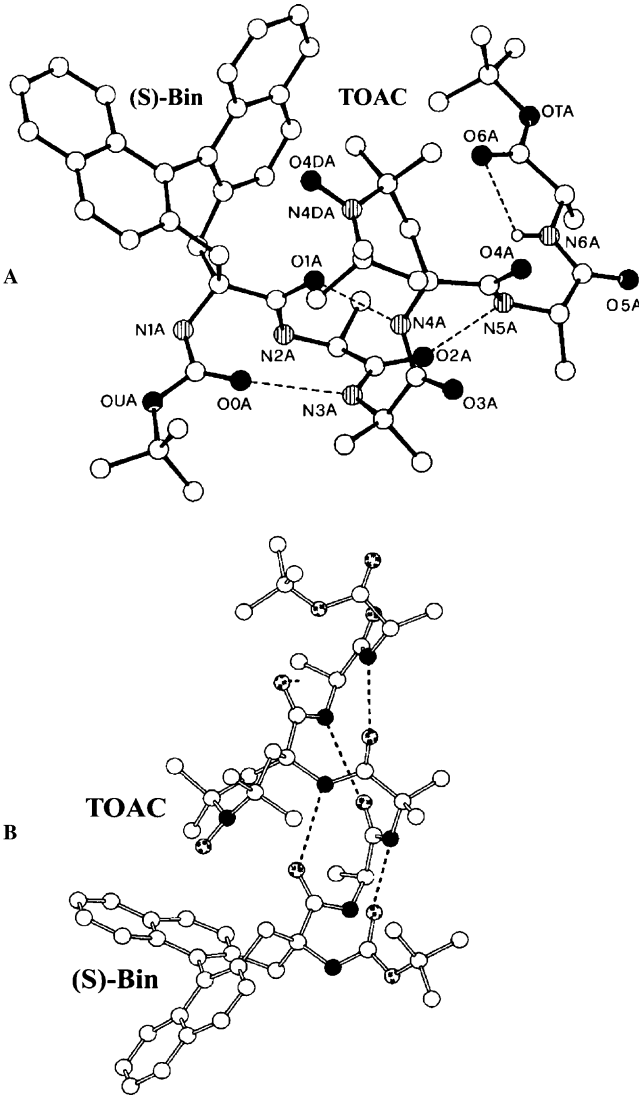

Figure 17. (A) X-ray diffraction structure of one of the two independent molecules in the asymmetric unit of Boc-(*S*)-Bin-L-Ala-Aib-TOAC-(L-Ala)$_2$-O*t*Bu (side view). Nitrogen and oxygen atoms are labeled. The intramolecular C=O···H—N H-bonds are represented by dashed lines [25b]. (B) Molecular model of the sterically most favored conformer of Boc-(*S*)-Bin-L-Ala-Aib-TOAC-(L-Ala)$_2$-O*t*Bu [25d]. The peptide main chain in the left-handed 3_{10}-helix is viewed perpendicularly to the helix axis. The four intramolecular C=O···H—N H-bonds are indicated by dashed lines. Nitrogen atoms are in black and oxygen atoms are dotted. Note the peculiarity of the handedness of the ordered backbone, which is not controlled by the chirality of the L-Ala residues, but rather by the chirality of the (*S*)-binaphthyl moiety at the N-terminus of the main chain. Note also the close approach of one methyl group of TOAC to one naphthyl moiety of Bin, forcing the chromophore to experience C—H···π interactions that stiffen the whole molecule.

chemistry. TOAC, likewise its prototype Aib, is a strong inducer of β-bend and 3_{10}-helical conformations [23a,b, 25b] (Figures 16A, B and 17A). Also, TOAC: (i) is able to undergo a nitroxide-based redox process (see above the section *Catalysis*) that can be monitored by cyclic voltammetry [23b]; and (ii) being a free radical, is responsible for dramatic quenching effects of suitably designed, fluorescence labeled peptides [25].

In the last few years, we took advantage of the properties of TOAC by extensively investigating (side-chain) donor–acceptor (side-chain) 3_{10}-helical peptide templates. Peptides either soluble in organic solvents or in aqueous solution were studied. The systems examined were of the (*i*)TOAC$\cdots$Xxx ($i+n$) type, with Xxx = TOAC, axially chiral Bin (Figure 3) or Trp. The N-terminal , 3_{10}-helical segment (positions 1 and 4) of the membrane-active, lipopeptaibol antibiotic trichogin GAIV was also probed with two TOAC residues [23f,g].

Hexameric peptides of general formula -TOAC-(L-Ala)$_n$-TOAC-(Ala)$_{4-n}$- ($n = 0$–3) were synthesized and studied by ESR in a number of alcohols of different polarities. Biradical J-coupling, reflecting the strength of TOAC$\cdots$TOAC interaction within each peptide, were used to determine the solvent-dependent peptide conformation. While the TOAC residues favor the 3_{10}-helix, our data demonstrated that they are unable to 'lock in' the helical structure. The incorporation of TOAC in water-soluble, N^{α}-acetylated 16-mer peptide amides provided a unique ESR signature, useful for distinguishing 3_{10}-helix from α-helix [23c,h]. The ESR study of the TOAC^{1,4} analogue of the 11-residue trichogin GA IV clearly showed that the lipopeptaibol secondary structure in solution survives essentially unchanged if compared to that found in the crystal state [23f,g]. More specifically, the N-terminal region of the peptide folds in a 3_{10}-helix.

The intramolecular quenching of photoexcited triplet state by a free radical linked to a peptide template was studied by time-resolved ESR with pulsed laser excitation. The systems investigated were 3_{10}-helix forming peptides, having in the amino acid sequence the free radical TOAC and a triplet precursor, such as Bin, Bpa, or Trp, incorporated at different relative positions [24]. Upon interaction with the excited triplet the TOAC radical spin sublevel populations assume values that differ from tha Boltzmann equilibrium values. This spin polarization effect produces ESR lines in emission, the time evolution of which reflects the triplet quenching rate. In particular, in a series of heptapeptides labeled with Bpa and TOAC at various positions in the 3_{10}-helix, a radical–triplet interaction was observed in all cases [24c]. However, for the peptide where Bpa and TOAC are at positions 2 and 4 the rate of triplet quenching is lower than that for the other peptides in the series. In addition, a radical–excited triplet complex in the quartet spin state was observed in a pentapeptide containing fullerene, as a triplet precursor, and TOAC [24a]. A CIDEP analysis of two hexapeptides, each characterized by either a Bpa or a Bin residue at position 1, and a TOAC residue at position 4, after one complete turn of the 3_{10}-helix, revealed that an intramolecular, though-space (rather than through-bond) interaction is operative [24b]. The observation of spin polarization makes the two helical hexapeptides suitable models to test the possibility of application of this novel spectroscopic technique to conformational studies of peptides in solution.

The terminally protected hexamer -(S)-Bin-L-Ala-Aib-TOAC-(L-Ala)$_2$- is the first peptide investigated photophysically that is characterized by: (a) a *rigid* α-amino acid fluorophore (Bin), (b) a *rigid* interchromophore bridge, the -Ala-Aib- sequence, and (c) a *rigid* α-amino acid quencher (TOAC) [25b]. In the crystal state, the backbone of the spectroscopically critical 1–4 segment of both independent molecules in the asymmetric unit of the hexapeptide is folded in a regular, left-handed 3_{10}-helix (Figure 17A). The steady-state fluorescence spectra show a remarkable quenching of Bin emission by the TOAC residue located one

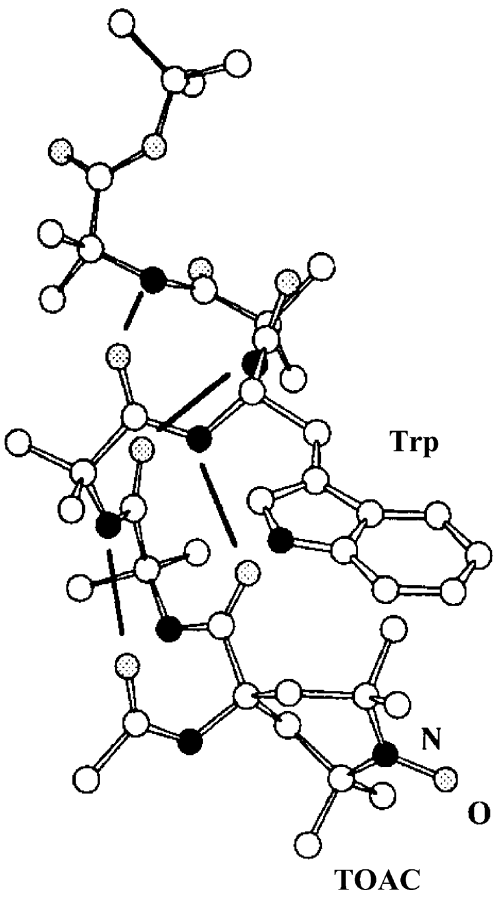

Figure 18. Molecular model of the deepest energy minimum structure of Ac-TOAC-(Aib)$_2$-L-Trp-(Aib)$_2$-O*t*Bu [25c]. The peptide main chain in the right-handed 3_{10}-helix is viewed perpendicularly to the helix axis. The four intramolecular C=O$\cdots$H—N H-bonds are indicated by dashed lines. Nitrogen atoms are in black and oxygen atoms are dotted.

complete turn of the helix apart. Time-resolved fluorescence measurements exhibit a bi-exponential decay with solvent-dependent lifetime components ranging from 0.5 to 1.5 and from 3 to 5 ns. Time-decay data combined with molecular mechanics calculations allowed us to assign these lifetimes to two left-handed 3_{10}-helical conformers in which an intramolecular energy transfer from excited Bin to TOAC takes place (Figure 17B). For a given solvent the difference between the two lifetimes primarily depends on a different relative orientation of the two chromophores in the conformers, which is in turn related to a different puckering of the TOAC cyclic system. In a related (R)-Bin/TOAC hexapeptide a right-handed 3_{10}-helix is that predominantly populated in solution [25d]. Therefore, in these two Bin-containing peptides the helical handedness is governed by the chirality of the atropoisomeric binaphtyl moiety rather than by that of the Ala residues. It is worth pointing out that the observed relationship between Bin chirality and peptide helix handedness is opposite to that shown by protein amino acids. The structural features of a series of 3_{10}-helical hexapeptides of general formula Boc-B-A_r-T-A_m-O*t*Bu, where A is L-Ala or Aib, B is (R)-Bin, T is TOAC, and $r + m = 4$, were recently investigated [25e]. These peptides are denoted as B-T/*r*-*m*, to emphasize the different position of TOAC with respect to that of the Bin fluorophore in the amino acid sequence. The rigidity of the B-T donor–acceptor pair and of the Aib-rich backbone allowed us to investigate the influence of the intercromophoric distance and orientation on the photophysics of the peptides examined. The excited state relaxation processes of binaphthyl were investigated by time-resolved fluorescence and transient absorption experiments. Dynamic quenching of the excited singlet state of binaphthyl by TOAC was successfully interpreted by the Förster energy transfer model, provided that the mutual orientation of the chromophores is taken into account. By comparison of the experimental and theoretical data, the type of secondary structure (right-handed 3_{10}-helix) for the B-T/*r*-*m* peptides was determined. This result would not have been achievable by using CD and NMR techniques only, as these are not diagnostic in this case. Static quenching was observed in all peptides examined but B-T/1-3, where the effect can be ascribed to a non-fluorescent complex. Among the computed low-energy conformers of these peptides, there is one structure exhibiting a N—O···— naphthalene center-to-center distance < 6 Å, which might be assigned to this complex.

3_{10}-Helical, Aib-based hexapeptides of general formula Ac-TOAC-$(Aib)_n$-L-Trp-$(Aib)_r$-O*t*Bu [T$(Aib)_n$Trp], where $n + r = 4$, were investigated by steady-state and time-resolved fluorescence measurements [25a,c]. Whatever the solvent, quenching of the excited Trp exhibits three lifetime components and proceeds on a time scale from subnanoseconds to a few nanoseconds. In all cases the fluorescence results are satisfactorily described by a dipole–dipole interaction mechanism, in which energy transfer takes place from the excited Trp to TOAC. This conclusion implies that interconversion among conformational substates is slow on the time scale of the transfer process, allowing us to estimate the dynamics of the process. Molecular mechanics calculations, coupled with time decay data, made it possible to build up the most probable structures of these 3_{10}-helical peptides (Figure 18).

Conclusions

Rigid molecular platforms provide well-defined distances and orientations between appropriate probes or functional groups, thus greatly facilitating a reliable and correct interpretation of experimental results based on the 3D-structural dependence of physical processes. Peptide-based systems of different lengths present a remarkable advantage over other types of derivatized skeletons because they are easily synthetically assembled.

Oligopeptides helices of variable length have already been used as templates. However, particularly in the case of relatively short peptides, only restricted mobility has been achieved. The most commonly used oligopeptide series in this context are (L-Pro)$_n$, followed by (Gly)$_n$, (L-Ala)$_n$, and γ-substituted (L-Glu)$_n$. Extensive investigations on (L-Pro)$_n$ oligomers have clearly shown that different populations of multiple conformers arise from *cis* ⇆ *trans* (ω torsion angle) and *cis*′⇆*trans*′ (ψ torsion angle) equilibria. On the other hand, (Gly)$_n$ oligomers are known to fold either in the ternary helix poly(Gly)$_n$ I or in the antiparallel β-sheet conformation poly(Gly)$_n$ II, while (L-Ala)$_n$ and γ-substituted (L-Glu)$_n$ oligomers may adopt either the α-helical or the β-sheet conformation. In addition, statistically unordered forms occur largely in the complex conformational equilibria of short oligopeptides from C^{α}-trisubstituted (protein) amino acids, with their population inversely proportional to the peptide main-chain length.

As it is clear that none of the peptide series discussed above can produce truly rigid backbone templates, in the last few years we concentrated our efforts on oligomeric series rich in the structurally restricted C^{α}-tetrasubstituted α-amino acids. After careful investigations of model compounds in both solution and crystal state, it was found that in short peptides rich in Aib, the parent compound, and in many other members of this family of amino acids, stable type-III′, β-bends and regular 3_{10}-helices are formed [12b]. This property largely depends, however, on the peptide main-chain length and C^{α}-tetrasubstituted α-amino acid content.

Nevertheless, most investigations have exploited as probes or reactive pendants: (a) flexible, unmodified, protein amino acids (His, Trp, Tyr, Cys, Met, Glu, Asp, Ser) or (b) flexible, appropriately side-chain modified, protein amino acids (Cys, Ser, Lys, Glu,

Asp, Ala, Pro, Phe). Although a limited side-chain flexibility might in general be tolerated, or may even be beneficial, that arising from all protein amino acids is definitely too large, making any conclusion unacceptably approximate. In other words, by utilizing this type of side chains any investigation inevitably suffers a range of uncertainty even larger than that saved from the restrictions imposed by rigidification of the backbone. As a consequence, side-chain rigidified fluorophores such as Bin and free radicals (or quenchers) such as TOAC are highly recommended when using main-chain conformationally restricted peptides as templates. In any case, the present review article clearly shows that to further expand this research direction (bend and helix-forming peptides as templates) a larger armamentarium of side-chain and main-chain constrained amino acids is needed.

Acknowledgements

The authors wish to thank Prof. P. Scrimin, Prof. A. Maggini, and Prof. C. Corvaja (University of Padova), Prof. E. Benedetti (University of Naples), Prof. B. Pispisa (University of Rome "Tor Vergata"), Prof. G. L. Millhauser (University of California, Santa Cruz), and their coworkers for productive collaborations.

References

1. (a) C. Toniolo, F. Formaggio, M. Crisma, G. Valle, W.H.J. Boesten, H.E. Schoemaker, J. Kamphuis, P.A. Temussi, E.L. Becker, and G. Précigoux: *Tetrahedron* **49**, 3641 (1993). (b) C. Toniolo, A. Bianco, F. Formaggio, M. Crisma, G.M. Bonora, E. Benedetti, V. Del Duca, M. Saviano, B. Di Blasio, C. Pedone, and A. Aubry: *Bioorg. Med. Chem.* **3**, 1211 (1995). (c) M. Crisma, A. Bianco, F. Formaggio, C. Toniolo, and J. Kamphuis: *Lett. Pept. Sci.* **2**, 187 (1995).
2. (a) C.M. Venkatachalam: *Biopolymers* **6**, 1425 (1968). (b) C. Toniolo: *CRC Crit. Rev. Biochem.* **9**, 1 (1980). (c) G.D. Rose, L.M. Gierasch, and J.A. Smith: *Adv. Protein Chem.* **37**, 1 (1985).
3. (a) C. Toniolo and E. Benedetti: *Trends Biochem. Sci.* **16**, 350 (1991). (b) D.J. Barlow and J.M. Thornton: *J. Mol. Biol.* **201**, 601 (1988). (c) I.L. Karle and P. Balaram: *Biochemistry* **29**, 6747 (1990). (d) M.E. Karpen, P.L. de Haseth, and K.E. Neet: *Protein Sci.* **1**, 1333 (1992). (e) G.L. Millhauser: *Biochemistry* **34**, 3873 (1995). (f) K.A. Bolin and G.L. Millhauser: *Acc. Chem. Res.* **32**, 1027 (1999). (g) L. Pal and G. Basu: *Protein Eng.* **12**, 811 (1999). (h) L. Pal, G. Basu, and P. Chakrabarti: *Proteins: Struct. Funct. Genet.* **48**, 571 (2002). (i) L. Pal, P. Chakrabarti, and G. Basu: *J. Mol. Biol.* **326**, 273 (2003).
4. (a) E. Benedetti, A. Bavoso, B. Di Blasio, V. Pavone, C. Pedone, C. Toniolo, and G.M. Bonora: *Proc. Natl. Acad. Sci. USA* **79**, 7951 (1982). (b) R. Nagaraj and P. Balaram: *Acc. Chem. Res.* **14**, 356 (1981). (c) S. Rebuffat, C. Goulard, B. Bodo, and M.-F. Roquebert: *Recent Res. Devel. Org. Biorg. Chem.* **3**, 65 (1999). (d) C. Toniolo, M. Crisma, F. Formaggio, C. Peggion, A.F. Epand, and R.M. Epand: *Cell. Mol. Life Sci.* **58**, 1179 (2001). (e) C. Peggion, F. Formaggio, M. Crisma, R.F. Epand, R.M. Epand, and C. Toniolo: *J. Pept. Sci.* **9**, 679 (2003).
5. H.S. Taylor: *Proc. Am. Phyl. Soc.* **85**, 1 (1941).
6. L. Pauling, R.B. Corey, and H.R. Branson: *Proc. Natl. Acad. Sci. USA* **37**, 205 (1951).
7. L. Bragg, J.C. Kendrew, and M.F. Perutz: *Proc. R. Soc. London* **A203**, 321 (1950).
8. (a) V. Pavone, G. Gaeta, A. Lombardi, F. Nastri, O. Maglio, C. Isernia, and M. Saviano: *Biopolymers* **38**, 705 (1996). (b) R.T. Wintjens, M.J. Rooman, and S.J. Wodak: *J. Mol. Biol.* **255**, 235 (1996). (c) K.-L. Chou: *Biopolymers* **42**, 837 (1997). (d) C. Ramakrishnan and D.V. Nataraj: *J. Pept. Sci.* **4**, 239 (1998).
9. (a) M.L. Huggins: *Chem. Rev.* **32**, 195 (1943). (b) J. Donohue: *Proc. Natl. Acad. Sci. USA* **39**, 470 (1953). (c) G.N. Ramachandran, C.M. Venkatachalam, and S. Krimm: *Biophys. J.* **66**, 849 (1966). (d) E.N. Baker and R.E. Hubbard: *Progr. Biophys. Mol. Biol.* **44**, 97 (1984).
10. (a) M. Marino, L. Braun, P. Cossart, and P. Ghosh: *Mol. Cell.* **4**, 1063 (1999). (b) M. Marino, L. Braun, P. Cossart, and P. Ghosh: *Proc. Natl. Acad. Sci. USA* **4**, 8784 (2000). (c) J.W. Peters, M.H.B. Stowell, and D.C. Rees: *Nature: Struct. Biol.* **3**, 991 (1996). (d) B. Kobe: *Nature: Struct. Biol.* **3**, 977 (1996). (e) B. Kobe and A.V. Kajava: *Trends Biochem. Sci.* **25**, 509 (2000). (f) B. Kobe and A.V. Kajava: *Curr. Opin. Struct. Biol.* **11**, 725 (2001). (g) A.V. Kajava and B. Kobe: *Protein Sci.* **11**, 1082 (2002).
11. G.R. Marshall: In N. Kharasch (ed.), *Intra-Science Chemistry Report (Vol. 5)*, Gordon and Breach (1971), pp. 305–316.
12. (a) N. Shamala, R. Nagaraj, and P. Balaram: *J. Chem. Soc., Chem. Commun.* 996 (1978). (b) C. Toniolo, M. Crisma, F. Formaggio, and C. Peggion: *Biopolymers (Pept. Sci.)* **60**, 396 (2001).
13. (a) V. Pavone, B. Di Blasio, A. Santini, E. Benedetti, C. Pedone, C. Toniolo, and M. Crisma: *J. Mol. Biol.* **214**, 633 (1990). (b) C. Toniolo, M. Crisma, G.M. Bonora, E. Benedetti, B. Di Blasio, V. Pavone, C. Pedone, and A. Santini: *Biopolymers* **31**, 129 (1991). (c) R. Gessmann, H. Brueckner, and K. Petratos: *J. Pept. Sci.* **9**, 753 (2003).
14. (a) M. Goodman, C. Toniolo, and P. Pallai: In B. Castro and J. Martinez (eds.), *Forum Peptides*, Dohr (1985), pp. 146-174. (b) V. Pavone, E. Benedetti, B. Di Blasio, C. Pedone, A. Santini, A. Bavoso, C. Toniolo, M. Crisma, and L. Sartore: *J. Biomol. Struct. Dyn.* **7**, 1321 (1990). (c) G.R. Marshall, E.E. Hodgkin, D.A. Langs, G.D. Smith, J. Zabrocki, and M.T. Leplawy: *Proc. Natl. Acad. Sci. USA* **87**, 487 (1990). (d) K. Okuyama, N. Tanaka, M. Doi, and M. Narita: *Bull. Chem. Soc. Jpn.* **61**, 3115 (1988).
15. C. Toniolo and E. Benedetti: *Macromolecules* **24**, 4004 (1991).
16. (a) C. Toniolo, G.M. Bonora, V. Barone, A. Bavoso, E. Benedetti, B. Di Blasio, P. Grimaldi, F. Lelj, V. Pavone, and C. Pedone: *Macromolecules* **18**, 895 (1985). (b) D.F. Kennedy, M. Crisma, C. Toniolo, and D. Chapman: *Biochemistry* **30**, 6541 (1991). (c) G. Yoder, A. Polese, R.A.G.D. Silva, F. Formaggio, M. Crisma, Q.B. Broxterman, J. Kamphuis, C. Toniolo, and T.A. Keiderling: *J. Am. Chem. Soc.* **119**, 10278 (1997). (d) C. Toniolo, A. Polese, F. Formaggio, M. Crisma, and J. Kamphuis: *J. Am. Chem. Soc.* **118**, 2744 (1996). (e) F. Formaggio, M. Crisma, P. Rossi, P. Scrimin, B. Kaptein, Q.B. Broxterman, J. Kamphuis and C. Toniolo: *Chem. Eur. J.* **6**, 4498 (2000). (f) R. Gratias, R. Konat, H. Kessler, M. Crisma, G. Valle, A. Polese, F. Formaggio, C. Toniolo, Q.B. Broxterman, and J. Kamphuis: *J. Am. Chem. Soc.* **120**, 4763 (1998). (g) S. Mammi, M. Rainaldi, M. Bellanda, E. Schievano, E. Peggion, Q.B. Broxterman, F. Formaggio, M. Crisma, and C. Toniolo: *J. Am. Chem. Soc.* **122**, 11735 (2000).
17. (a) F. Donald, G. Hungerford, D.J.S. Birch, and B.D. Moore: *Chem. Commun.* 313 (1995). (b) G. Hungerford, M. Martinez-Insua, D.J.S. Birch, and B.D. Moore: *Angew. Chem. Int. Ed. Engl.* **37**, 326 (1998). (c) P. Pengo, L. Pasquato, S. Moro, A. Brigo, F. Fogolari, Q.B. Broxterman, B. Kaptein, and P. Scrimin: *Angew. Chem. Int. Ed.* **42**, 3388 (2003).
18. (a) C.E. Schafmeister, J. Po, and G.L. Verdine: *J. Am. Chem. Soc.* **122**, 5891 (2000). (b) H.E. Blackwell and J.H. Grubbs: *Angew. Chem. Int. Ed. Engl.* **37**, 3281 (1998). (c) H.E. Blackwell, J.S. Sadowski, R.J. Howard, J.N. Sampson, J.A. Chao, W.E. Steinmetz, D.J. O' Leary, and R.H. Grubbs: *J. Org. Chem.* **66**, 5291 (2001). (d) S.J. Miller, H.E. Blackwell, and R.H. Grubbs: *J. Am. Chem. Soc.* **118**, 9606 (1996). (e) B. Kaptein, Q.B. Broxterman, H.E. Schoemaker, F.P.J.T. Rutjes, J.J.N. Veerman, J. Kamphuis, C. Peggion, F. Formaggio, and C. Toniolo: *Tetrahedron* **57**, 6567 (2001). (f) J. Pernerstorfer, M. Schuster, and S. Blechert: *J. Chem. Soc., Chem. Commun.* 1949 (1997). (g) A. Ravi, B.V. Venkataram Prasad, and P. Balaram:

J. Am. Chem. Soc. **105**, 105 (1983). (h) M. Saviano, E. Benedetti, R.M. Vitale, B. Kaptein, Q.B. Broxterman, M. Crisma, F. Formaggio, and C. Toniolo: *Macromolecules* **35**, 4204 (2002).

19. F. Formaggio, M. Bonchio, M. Crisma, C. Peggion, S. Mezzato, A. Polese, A. Barazza, S. Antonello, F. Maran, Q.B. Broxterman, B. Kaptein, J. Kamphuis, R.M. Vitale, M. Saviano, E. Benedetti, and C. Toniolo: *Chem. Eur. J.* **8**, 84 (2002).
20. (a) S.J. Miller, G.T. Copeland, N. Papaioannou, T.E. Horstmann, and E.M. Ruel: *J. Am. Chem. Soc.* **120**, 1629 (1998). (b) G.T. Copeland, E.R. Jarvo, and S.J. Miller: *J. Org. Chem.* **63**, 6784 (1998). (c) G.T. Copeland and S.J. Miller: *J. Am. Chem. Soc.* **121**, 4306 (1999). (d) E.R. Jarvo, G.T. Copeland, N. Papaioannou, P.J. Bonitatebus, Jr., and S.J. Miller: *J. Am. Chem. Soc.* **121**, 11638 (1999). (e) R.F. Harris, A.J. Nation, G.T. Copeland, and S.J. Miller: *J. Am. Chem. Soc.* **122**, 11270 (2000). (f) J.T. Blank, D.J. Guerin, and S.J. Miller: *Org. Lett.* **2**, 1247 (2000). (g) E.R. Jarvo, M.M. Vasbinder, and S.J. Miller: *Tetrahedron* **56**, 9773 (2000). (h) M.M. Vasbinder, E.R. Jarvo, and S.J. Miller: *Angew. Chem. Int. Ed.* **40**, 2824 (2001). (i) G.T. Copeland and S.J. Miller: *J. Am. Chem. Soc.* **123**, 6496 (2001). (j) E.R. Jarvo, C.A. Evans, G.T. Copeland, and S.J. Miller: *J. Org. Chem.* **66**, 5522 (2001).
21. (a) P. Rossi, F. Felluga, P. Tecilla, F. Formaggio, M. Crisma, C. Toniolo, and P. Scrimin: *J. Am. Chem. Soc.* **121**, 6948 (1999). (b) P. Rossi, F. Felluga, P. Tecilla, F. Formaggio, M. Crisma, C. Toniolo, and P. Scrimin: *Biopolymers (Pept. Sci.)* **55**, 496 (2000). (c) C. Sissi, P. Rossi, F. Felluga, F. Formaggio, M. Palumbo, P. Tecilla, C. Toniolo, and P. Scrimin: *J. Am. Chem. Soc.* **123**, 3169 (2001). (d) A. Scarso, U. Scheffer, M. Göbel, Q.B. Broxterman, B. Kaptein, F. Formaggio, C. Toniolo, and P. Scrimin: *Proc. Natl. Acad. Sci. USA* **99**, 5144 (2002).
22. (a) M. Maggini, G. Scorrano, A. Bianco, and C. Toniolo: *J. Chem. Soc., Chem. Commun.* 305 (1994). (b) A. Bianco, F. Gasparrini, M. Maggini, D. Misiti, A. Polese, M. Prato, G. Scorrano, C. Toniolo, and C. Villani: *J. Am. Chem. Soc.* **119**, 7550 (1997). (c) A. Bianco, C. Corvaja, M. Crisma, D.M. Guldi, M. Maggini, E. Sartori, and C. Toniolo: *Chem. Eur. J.* **8**, 1544 (2002). (d) S.H. Friedman, D.L. De Camp, R.P. Sijbesma, G. Srdanov, F. Wudl, and G.L. Kenyon: *J. Am. Chem. Soc.* **115**, 6506 (1993). (e) A. Bianco, T. Da Ros, M. Prato, and C. Toniolo: *J. Pept. Sci.* **7**, 208 (2001).
23. (a) C. Toniolo, M. Crisma, and F. Formaggio: *Biopolymers (Pept. Sci.)* **47**, 153 (1998). (b) C. Toniolo, E. Valente, F. Formaggio, M. Crisma, G. Pilloni, C. Corvaja, A. Toffoletti, G.V. Martinez, M.P. Hanson, G.L. Millhauser, C. George and J.L. Flippen-Anderson: *J. Pept. Sci.* **1**, 45 (1995). (c) P. Hanson, G. Martinez, G. Millhauser, F. Formaggio, M. Crisma, C. Toniolo, and C. Vita: *J. Am. Chem. Soc.* **118**, 271 (1996). (d) P. Hanson, G. Millhauser, F. Formaggio, M. Crisma, and C. Toniolo: *J. Am. Chem. Soc.* **118**, 7618 (1996). (e) P. Hanson, D.J. Anderson, G. Martinez, G. Millhauser, F. Formaggio, M. Crisma, C. Toniolo, and C. Vita: *Mol. Phys.* **95**, 957 (1998). (f) V. Monaco, F. Formaggio, M. Crisma, C. Toniolo, P. Hanson, G. Millhauser, C. George, J.R. Deschamps, and J.L. Flippen-Anderson: *Bioorg. Med. Chem.* **7**, 119 (1999). (g) D.J. Anderson, P. Hanson, J. Mc Nulty, G. Millhauser, V. Monaco, F. Formaggio, M. Crisma, and C. Toniolo: *J. Am. Chem. Soc.* **121**, 6919 (1999). (h) J.C. Mc Nulty, J.L. Silapie, M. Carnevali, C.T. Farrar, R.G. Griffin, F. Formaggio, M. Crisma, C. Toniolo, and G.L. Millhauser: *Biopolymers* (*Pept. Sci.*) **55**, 479 (2000).
24. (a) C. Corvaja, E. Sartori, A. Toffoletti, F. Formaggio, M. Crisma, and C. Toniolo: *Biopolymers (Pept. Sci.)* **55**, 486 (2000). (b) C. Corvaja, E. Sartori, A. Toffoletti, F. Formaggio, M. Crisma, C. Toniolo, J.-P. Mazaleyrat, and M. Wakselman: *Chem. Eur. J.* **6**, 2775 (2000). (c) E. Sartori, A. Toffoletti, F. Rastrelli, C. Corvaja, A. Bettio, F. Formaggio, S. Oancea, and C. Toniolo: *J. Phys. Chem.* **A107**, 6905 (2003).
25. (a) B. Pispisa, A. Palleschi, L. Stella, M. Venanzi, and C. Toniolo: *J. Phys. Chem.* **B102**, 7890 (1998). (b) C. Toniolo, F. Formaggio, M. Crisma, J.-P. Mazaleyrat, M. Wakselman, C. George, J.R. Deschamps, J.L. Flippen-Anderson, B. Pispisa, M. Venanzi, and A. Palleschi: *Chem. Eur. J.* **5**, 2254 (1999). (c) B. Pispisa, L. Stella, M. Venanzi, A. Palleschi, F. Marchiori, A. Polese, and C. Toniolo: *Biopolymers* **53**, 169 (2000). (d) B. Pispisa, C. Mazzuca, A. Palleschi, L. Stella, M. Venanzi, F. Formaggio, C. Toniolo, J.-P. Mazaleyrat, and M. Wakselman: *J. Fluoresc.* **13**, 139 (2003). (e) B. Pispisa, C. Mazzuca, A. Palleschi, L. Stella, M. Venanzi, M. Wakselman, J.-P. Mazaleyrat, M. Rainaldi, F. Formaggio, and C. Toniolo: *Chem. Eur. J.* **9**, 4084 (2003).